



Moisture sorption isotherms, thermodynamic properties and sorption properties of walnut flavor microcapsules

Isotermas de adsorción de humedad, propiedades termodinámicas y propiedades de adsorción de microcápsulas de saborizante de nuez

S.K. Velázquez-Gutiérrez¹, A. Román-Guerrero², S. Cortés-Camargo³, J. Cruz-Olivares¹, M.F. Fabela-Morón^{1,4}, C. Pérez-Alonso^{1*}

¹Departamento de Ingeniería Química, Facultad de Química, Universidad Autónoma del Estado de México, Paseo Colón esq. Paseo Tollocan s/n, Col. Residencial Colón, C.P. 50120, Toluca, Estado de México, México.

²Departamento de Biotecnología, Universidad Autónoma Metropolitana-Iztapalapa, Ferrocarril San Rafael Atlixco No. 186, Col. Leyes de Reforma 1ª Sección, C.P. 09310, Ciudad de México, México.

³Departamento de Nanotecnología, Universidad Tecnológica de Zinacantepec, Av. Libramiento Universidad 106, Col. San Bartolo el Llano, C.P. 51361, Zinacantepec, Estado de México, México.

⁴Departamento de Ciencias de la Alimentación, Universidad Autónoma Metropolitana-Lerma, Av. De las Garzas No. 10, Col. El Panteón, C.P. 52005, Lerma de Villada, Estado de México, México.

Received: April 4, 2024; Accepted: June 14, 2024

Abstract

Flavorings are encapsulated through spray drying to ensure protection throughout their shelf life. However, the stability of microencapsulated flavorings largely depends on the choice of wall material. This work evaluates three wall material systems of walnut flavor: microcapsules of mesquite gum (M_{MG}), whey protein concentrate (M_{WPC}) and a 1:1 (w:w) mixture of both (M_{MG-WPC}), onto their moisture sorption isotherms, fitting to GAB model, thermodynamic and sorption properties at different temperatures (25, 35 and 40°C). The M_{MG} displayed greater monolayer moisture adsorption capacity (M_0 : 4.69-5.52 kg H₂O/100 kg dried solid (d.s.)) and adsorbent-adsorbate interaction due to its greater hygroscopicity, but less tendency to agglomeration trend than M_{WPC} and M_{MG-WPC} . The M_{MG} exhibited the lowest differential enthalpy and entropy values, promoting an advantageous dehydration process and ensuring greater stability, which was attributed to the enhancement of water molecular order. Additionally, M_{MG} displayed the largest sorption surface area, facilitating the moisture sorption process. Therefore, all three microcapsules' systems were able to stabilize the walnut flavor, however, their slight differences in their moisture sorption capacity led to different stabilization mechanisms that affected their shelf life.

Keywords: Walnut flavoring; Microcapsules; Moisture sorption isotherms; Thermodynamics.

Resumen

Los saborizantes se encapsulan mediante secado por aspersión para asegurar su protección durante la vida de anaquel. Sin embargo, la estabilidad de los saborizantes microencapsulados depende en gran medida del material de pared seleccionado. Este trabajo evalúa tres sistemas de materiales de pared en la encapsulación de saborizante de nuez: microcápsulas de goma de mezquite (M_{MG}), concentrado de proteína de suero de leche (M_{WPC}) y una mezcla 1:1 (p:p) de ambos materiales (M_{MG-WPC}), respecto a sus isotermas de adsorción y ajuste al modelo de GAB, termodinámica y propiedades de adsorción a diferentes temperaturas de (25, 35 y 40°C). Las microcápsulas M_{MG} mostraron valores más altos de humedad en la monocapa (M_0 : 4.69-5.52 kg H₂O/100 kg sólido seco (s.s.)) y mayor interacción adsorbente-adsorbato debido a su higroscopicidad y menor tendencia a aglomerarse que las microcápsulas M_{WPC} y M_{MG-WPC} . Las M_{MG} presentaron los valores más bajos de entalpía y entropía diferencial, promoviendo y beneficiando el proceso de deshidratación y asegurando mayor estabilidad al fomentar un mejor orden de las moléculas del agua sobre el material de pared. Adicionalmente, M_{MG} mostraron mayor área superficial de adsorción en comparación con los otros sistemas, facilitando el proceso de adsorción de agua. Por lo tanto, los tres sistemas de microcápsulas fueron capaces de estabilizar el saborizante de nuez, aunque existen pequeñas diferencias en la capacidad de adsorción de humedad que conllevan a tener diferentes mecanismos de estabilización que afectan su vida de anaquel.

Palabras clave: Saborizante de nuez; Microcápsulas; Isotermas de adsorción; Termodinámica.

* Corresponding author. E-mail: cpereza@uaemex.mx;

<https://doi.org/10.24275/rmiq/Alim24307>

ISSN:1665-2738, issn-e: 2395-8472

1 Introduction

Food flavors usually comprise volatile compounds added into food and beverages to influence the perception of human senses for imparting specific tastes and aromas and improving the acceptability and sales (Saffarionpour, 2019; Sultana *et al.*, 2018). Flavors can be sensitive to different environmental and physicochemical factors such as pH, humidity, temperature, acid and basic media, oxygen, light, and enzymatic reactions, leading to potential degradation and loss of intensity, as well as developing modified undesirable flavors. Despite these challenges, ongoing research is focused on minimizing these issues and enhancing their use by providing adequate protection during the processing, storage, and shelf life of processed foods (Saifullah *et al.*, 2019; Kim *et al.*, 2019; Feng *et al.*, 2018; Fuciños *et al.*, 2017). Hence, there exists a demand and keen interest in encapsulating food flavors to preserve their inherent qualities and mitigate their drawbacks (Premjit *et al.*, 2022).

Encapsulation is an efficient technology that serves to increase the stability of flavorings contributing to reducing their degradation, improving the functionality of the encapsulated products (size, structure, and shape of the particles), and allowing easier handling and controlled release of the flavor. Different encapsulation technologies can be applied to produce flavor encapsulation systems, utilizing a wide variety of encapsulating agents such as gums, maltodextrins, starches, and proteins (Carneiro *et al.*, 2022; Samakradhamrongthai *et al.*, 2019). Among the encapsulation technologies widely utilized for ensuring the protection, stability, and shelf life of flavorings, prominent methods include the spray drying, ionic gelation, fluidization bed coating, extrusion, and spray cooling (Saini *et al.*, 2020).

One of the major concerns in the microencapsulation process is the focus on the development of analytical methods that can predict optimal storage conditions to ensure *a priori*, the long-term stability of spray-dried microcapsules. In this sense, water sorption isotherms have been used with great success to determine the storage stability of dehydrated foods and to predict their shelf life, allowing not only to characterize the moisture sorption mechanisms, critical level of moisture, and interactions occurred between the components of the food solid matrix and water (Hernández-Carrillo *et al.*, 2019; Shanker *et al.*, 2019; Soleimanifard & Hamdami, 2018; Gallegos-Marin *et al.*, 2016), but also the relationship between water activity (a_w) and equilibrium moisture content (M) at constant conditions of temperature and pressure (Osorio-Tellez *et al.*, 2021; Pascual-Pineda *et al.*, 2017). They can

provide valuable insights into structural changes within the microencapsulation matrix resulting from water vapor diffusion, such as collapse, shrinkage, stickiness, and other detrimental effects that threaten the stability of the core material. Additionally, these observations offer guidance for determining optimal packaging and storage conditions (Collazos-Escobar *et al.*, 2022; De Araújo & Da Silva-Pena, 2022; Velázquez-Gutiérrez *et al.*, 2021).

The objective of this work was to produce walnut flavor microcapsules by spray drying using different wall materials (mesquite gum (MG), whey protein concentrate (WPC), and 1:1 of MG:WPC mixture), evaluating their water sorption isotherms and applying the GAB model to determine sorption and thermodynamic properties, such as differential enthalpy, entropy, and Gibbs free energy. These properties are crucial for the understanding of the mechanisms underlying water vapor adsorption and microstructural changes in the spray-dried microcapsules.

2 Materials and methods

2.1 Materials

The walnut flavoring was kindly donated by the company Sensient Colors S.A. of C.V. (Toluca, State of Mexico). Universidad Autónoma de Nuevo León (Dr. J.G. Báez-González) provided the mesquite gum powder (MG) obtained from *Prosopis laevigata* trees. Whey protein concentrate (WPC, 80% protein in dry basis (d.b.)) was obtained from the company Hilmar Ingredients (California, USA). These hydrocolloids were used as encapsulating agents. At SIGMA Aldrich, S.A. of C.V. (Mexico), deionized water and chemical reagents were purchased to carry out the different experimental tests.

2.2 Experimental methods

2.2.1 Preparation of walnut flavor microcapsules

Stock solutions of MG, WPC and a mixture of MG-WPC (1:1 mass ratio) were prepared at room temperature and kept under constant stirring (12 h) to hydrate hydrocolloids fully. Subsequently, nut flavoring was dissolved in the aqueous solutions until reaching a solids content of 28% w/w by homogenizing the systems with an Ultra-Turrax IKA T50 rotor-stator homogenizer (NC, USA) for 5 minutes at 10,000 rpm. The obtained emulsions were dehydrated in a Nichols/Niro (NY, USA) pilot plant spray dryer with a 5 mm needle atomizer at an air inlet temperature of 135 ± 5 °C, a pressure of 4 bar of compressed air, and a feed rate of 40 cm³/min. The

microcapsules produced were labeled as M_{MG} , M_{WPC} and M_{MG-WPC} (based on the wall material used in each case), collected, and stored in amber bottles at room temperature (~ 20 °C) until later use.

2.2.2 Sorption isotherms of microcapsules

Initially the microcapsules produced were conditioned in P_2O_5 for twenty days at room temperature to achieve a minimum moisture content ($\sim 2\%$). Subsequently, experimental adsorption isotherms at 25, 35 and 40 (± 0.1) °C throughout a water activity (a_w) range from 0.11 to 0.85 were determined by using the static-desiccator method. Approximately 1.0 g of microcapsules were placed in small glass desiccators of 10 cm diameter, containing saturated solutions of different salts that provided water activity values in the studied range of this thermodynamic parameter. The samples were weighed every two days until was reached a state of pseudo-equilibrium between the analyzed samples and the saturated solutions (Velázquez-Gutiérrez *et al.*, 2021).

Each kind of microcapsules were put into a vacuum drier whose temperature was fixed at 60 °C for 24 h, the equilibrium moisture content was registered when there was a difference < 0.001 g between three consecutive weight measurements, the hygroscopic equilibrium for microcapsules was reached approximately after 30 days. A water activity meter (model series 3 TE, Pullman, WA, USA) was used to measure the water activity. The experiments were conducted in three replicates. The moisture sorption isotherms of microcapsules were constructed by plotting equilibrium moisture content (M) vs water activity (a_w) obtained values at each temperature. Each point found in the conformation of each one of the isotherms was the result of the arithmetic average of three determinations carried out.

2.2.3 Particle microstructure

A scanning electron microscope (SEM) JSM-6510 model equipment (Jeol Co. Ltd., Tokyo, Japan) with the GB-H mode was used to obtain microcapsules morphology images under standard operating conditions. As the electron microscope operates under ultra-vacuum conditions, it was not necessary for the microcapsule samples to be metallized.

2.3 Theoretical methods

2.3.1 Modeling sorption isotherms by GAB equation

Guggenheim–Anderson–de Boer (GAB) mathematical theoretical model (Eq. 1) was used to describe the experimental moisture sorption isotherms

(Arslan-Tontul, 2021):

$$M = \frac{M_0CKa_w}{(1 - Ka_w)(1 - Ka_w + CKa_w)} \quad (1)$$

This equation was used due to its great versatility to adequately represent the experimental sorption data of foods and foodstuffs in a wide range of water activity (0.1-0.9) (Timmermann *et al.*, 2001). This theoretical model assumes that the states of the water molecules in the second and higher layer equal to each other, but different from those of the liquid state. Therefore, the GAB model introduces a second well-differentiated sorption stage for the water molecules. This assumption introduces a third parameter (K) that relates the difference in the sorbate's pure liquid state and the upper layers, having values between 0.7 and 1.0 (Quirijns *et al.*, 2005). The parameter C is related to the difference in magnitude between higher layers and the monolayer moisture content (M_0) (Timmermann, 1989).

The suitability of experimental data to model was estimated using the nonlinear optimization method Levenberg–Marquardt with the software OriginPro 8.5 (Origin Lab Corporation, Northampton, MA, USA). The most suitable sorption model was selected based on the coefficient of determination (R^2) and the mean relative error (E %) derived from the fit (Eq. 2). A fit was deemed satisfactory when the coefficient of determination exceeded 0.98 and the absolute percentage error remain below 5% (Silva *et al.*, 2021; Arslan-Tontul, 2021).

$$E(\%) = \frac{100}{n_s} \sum \frac{|M_i - M_{Ei}|}{M_i} \quad (2)$$

2.3.2 Differential thermodynamic properties of the microcapsules

Net isosteric heat of adsorption (q_{st}) or differential enthalpy (ΔH_{dif}) is defined as the difference between the heat of vaporization of water and the total heat of sorption. The determination of differential enthalpy involved applying the Clausius-Clapeyron equation (Eq. 3), assuming a constant moisture content in the adsorbent and an enthalpy of vaporization of pure water that remains unaffected by temperature (Arslan-Tontul, 2021; Pérez-Alonso *et al.*, 2006):

$$\left(\frac{\partial \ln a_w}{\partial \left(\frac{1}{T} \right)} \right)_M = - \frac{\Delta H_{dif}}{R} = - \frac{q_{st}}{R} \quad (3)$$

These assumptions are valid when the water vapor adsorption process (adsorbate) is carried out at relatively low (moderate) temperatures in the adsorbent (microcapsules).

The Gibbs-Helmholtz equation (Eq. 4) was utilized to calculate differential entropy (ΔS_{dif}) of

water sorption in microcapsules (Pérez-Alonso *et al.*, 2006):

$$\Delta S_{dif} = \frac{\Delta H_{dif}}{T} - R \ln a_w \quad (4)$$

The Gibbs equation (Eq. 5) was used to calculate the Gibbs free energy (ΔG); this gives information of the sorption process related to spontaneity and the affinity between adsorbent and water molecules (Rizvi, 1986):

$$\Delta G = RT \ln a_w \quad (5)$$

2.3.3 Compensation theory

A linear relationship ΔH_{dif} vs. ΔS_{dif} was obtained using the law of compensation (Eq. 6) to determine the dominating mechanisms (entropic and enthalpic) of the water adsorption process (Rosa *et al.*, 2021). The compensation theory is confirmed only when the isokinetic temperature (T_β) is different from the harmonic mean temperature (T_{hm}); this is calculated by Eq. 7 (Krug *et al.*, 1976a, 1976b).

$$\Delta H_{dif} = T_\beta \Delta S_{dif} + \Delta G_\beta \quad (6)$$

$$T_{hm} = \frac{n_i}{\sum_1^{n_i} \left(\frac{1}{T}\right)} \quad (7)$$

2.3.4 Sorption properties of microcapsules

A physical parameter that provides an insight into the bound water onto microcapsule surface is the sorption surface area (S_0) and it can be calculated by Eq. (8) considering the monolayer moisture content (M_0) obtained from the GAB model (Rosa *et al.*, 2021).

$$S_0 = M_0 \frac{1}{M_w} N_0 A_w = 3.5 \times 10^3 M_0 \quad (8)$$

Characterization of the pore structure of the microcapsule improves the understanding of the adsorption process because it affects the transport of water molecules. The critical radius (r_c) was calculated by the Kelvin equation (Eq. 9), which considers mainly the condensation region of the isotherm mainly (Singh *et al.*, 2001).

$$r_c = \frac{2\sigma V_M}{RT \ln\left(\frac{1}{a_w}\right)} \quad (9)$$

At a given water activity, the thickness of the layer produced on the porous surface was calculated using the Halsey equation (Eq. 10) (Velázquez-Gutiérrez *et al.*, 2021; Singh *et al.*, 2001):

$$t = 0.354 \left(\frac{-5}{\ln a_w} \right)^{\frac{1}{3}} \quad (10)$$

Thus, pore radius (R_p) was obtained according to Eq. (11) (Alpizar-Reyes *et al.*, 2017; Singh *et al.*, 2001):

$$R_p = 10^9 r_c + t \quad (11)$$

In micropores, the Dubinin-Radushkevich model (Eq. 12) is widely used because it considers a deviation from Kelvin-law since adsorbent interactions in these pores dominate the pore filling mechanism (Azuara & Beristain, 2006). According to this model, adsorption in micropores will follow a volume filling at low pressures and capillary condensate at higher pressures (multilayer region); for mesopores at low pressures, it will be a submonolayer region, and then a multilayer thickness of the adsorbate at higher pressures (Sonwane & Bhatia, 2000).

$$\log(M) = \log(M_{0D}) - b \cdot \log^2\left(\frac{1}{a_w}\right) \quad (12)$$

2.4 Statistical analyses

Measurements were conducted in triplicate for each test. ANOVA test and $P < 0.05$ (interval of confidence of 95%) were utilized for the statistical analysis and were performed by Minitab software (Minitab Inc., State College, PA, USA). Data fitting were carried out through Origin version 8.5 Scientific Graphing and Analysis Software (OriginLab Corp., Northampton, MA, USA).

3 Results and discussion

3.1 Sorption isotherms of microcapsules

Fig. 1 presents the experimental sorption isotherms of microcapsules at 25, 35 and 40 °C, it is observed that at a constant temperature, the equilibrium moisture content increased with water activity. It is also been shown that increasing temperature causes a reduction in sorptivity in the microcapsules due to the process's exothermicity. According to Brunauer classification, the curves were sigmoidal type II, characterized by substances with high molecular weight (Stępień *et al.*, 2020) and indicative of the possible presence of adsorption in multilayers, as well as monolayers, where relative humidity promotes the water sorption into porous and granular surfaces (Silva *et al.*, 2021). Isotherms of type II are formed by three zones, the first region ($a_w < 0.3$) is attributed to the monolayer moisture content where water molecules are strongly bound to the product matrix; the second zone ($0.3 < a_w < 0.7$) displays a curve almost linear and corresponds to the water of the multilayer; and the last zone ($a_w \geq 0.7$) indicates that water is filling the capillaries of the food and thus, modification of its properties to simulate those of free water is ready for use into microbiological and chemical reactions (Ociecek *et al.*, 2022; Silva *et al.*, 2021; Rosa *et al.*, 2021).

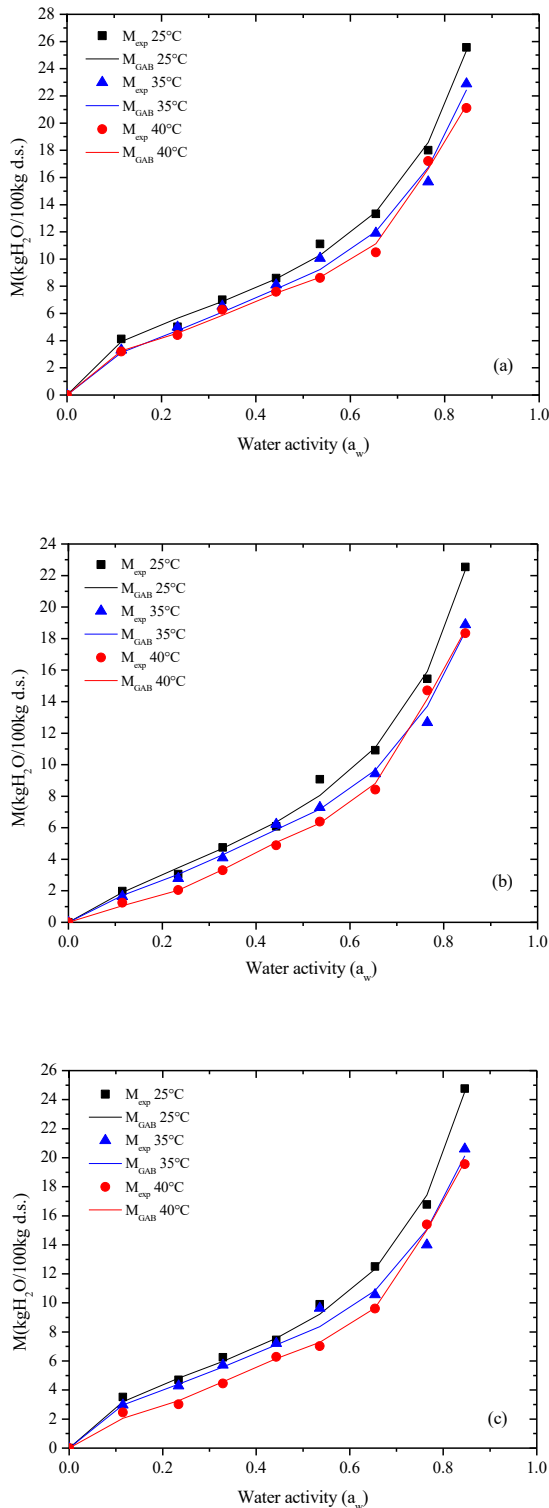


Figure 1. Water sorption isotherms of walnut flavor microcapsules at 25, 35 and 40 °C for (a) M_{MG} ; (b) M_{WPC} and (c) M_{MG-WPC} .

When the temperature increased, it was observed, which led a reduction in the number of active sites and physicochemical changes to a decrease in the equilibrium moisture content for all microcapsules. It was observed that M_{WPC} had slightly lower equilibrium moisture contents than the M_{MG} -based microcapsules, thus indicating the presence of more

quantity of insoluble moieties in the WPC, probably related to the hydrophobic aminoacids present in the protein, which reduces the water adsorption capacity of the biopolymer material (Włodarczyk-Stasiak & Jamroz, 2008).

Table 1 shows the GAB parameters obtained for the three microcapsules systems at temperatures of 25, 35, and 40 °C. The moisture content of the monolayer refers to the parameter used to quantify the amount of water strongly bound to the material's sorption sites. This parameter is where microbiological and biochemical degradation reactions are minimized, resulting in increased stability in dried materials (Hoyos-Leyva *et al.*, 2018; Velázquez-Gutiérrez *et al.*, 2015; Chranioti *et al.*, 2015). For the analyzed systems, the values of M_0 varied from 4.15 to 5.52 kg $H_2O/100$ kg d.s. The values of the moisture content of the monolayer reported by Bonilla *et al.* (2010) for canola oil encapsulated into mesquite gum and whey protein concentrate at 25 and 35 °C exhibited similarities to the findings of this study at corresponding temperatures.

The parameter C is related to adsorbent-adsorbate interactions, where higher C values indicate stronger binding. In this study, the M_{MG} microcapsules displayed higher values, while M_{WPC} showed lower values. This behavior can be attributed to the lower hygroscopicity of WPC compared to MG. The K parameter is related to absorbent-multilayer molecules interactions, K values for all three systems were very similar and close to 1, suggesting a free water behavior in the multilayer structure of the microcapsules (Quirijns *et al.*, 2005).

3.2 Particle microstructure

Fig. 2 illustrates the microstructure of (a) M_{MG} , (b) M_{WPC} , and (c) M_{MG-WPC} microcapsules. For M_{MG} , the microcapsules exhibited circular-shaped particles and irregular topology, featuring some dents and a generally smooth surface. This morphology is attributed to the inherent properties of mesquite gum which serves as wall material to encapsulate walnut flavoring, and to the process conditions through the utilization of a pressure nozzle in a parallel array of drying chamber, facilitating the formation of microdroplets that finally undergo drying to obtain powder-form microcapsules. During the spray drying process, microstructural imperfections arise as a consequence of water evaporation, leading to expansion and subsequent collapse of the wall material (Drusch & Berg, 2008). This characteristic microstructure also has been observed in microcapsules containing fish oil (Espinosa-Andrews *et al.*, 2022), *Hybiscus sabdariffa* extract (Ochoa-Velasco *et al.*, 2017), lemon essential oil (Cortés-Camargo *et al.*, 2017), orange peel oil

Table 1. Estimated GAB parameters for walnut flavor microcapsules.

| System | Parameters | 25 °C | 35 °C | 40 °C |
|--------------|------------|--------------------|----------------------|--------------------|
| M_{MG} | M_0 | 5.52 ± 0.32^a | 5.26 ± 0.28^{ab} | 4.69 ± 0.31^b |
| | C | 14.54 ± 0.62^a | 10.08 ± 0.51^a | 14.43 ± 0.63^b |
| | K | 0.93 ± 0.02^a | 0.94 ± 0.03^a | 0.99 ± 0.05^a |
| | R^2 | 0.998 | 0.999 | 0.999 |
| | E (%) | 4.07 | 4.96 | 2.92 |
| M_{WPC} | M_0 | 4.92 ± 0.25^a | 4.68 ± 0.22^{ab} | 4.79 ± 0.32^b |
| | C | 4.35 ± 0.34^a | 4.35 ± 0.42^a | 2.17 ± 0.52^b |
| | K | 0.94 ± 0.0^a | 0.93 ± 0.02^a | 0.98 ± 0.05^a |
| | R^2 | 0.996 | 0.997 | 0.997 |
| | E (%) | 4.98 | 4.72 | 3.97 |
| M_{MG-WPC} | M_0 | 4.92 ± 0.27^a | 4.71 ± 0.32^{ab} | 4.15 ± 0.41^b |
| | C | 11.18 ± 0.53^a | 11.62 ± 0.42^a | 6.82 ± 0.64^b |
| | K | 0.95 ± 0.02^a | 0.94 ± 0.09^a | 1.01 ± 0.08^a |
| | R^2 | 0.999 | 0.997 | 0.997 |
| | E (%) | 3.81 | 4.08 | 4.68 |

*MG: Mesquite gum; WPC: Whey protein concentrate; M_0 : Moisture content of the monolayer (kg water/100 kg d.s; C and K : GAB model constants; R^2 : Coefficient of linear determination; E : Mean relative deviation modulus (%).

**Results are presented as means \pm SD ($n=3$).

***Values with different letters in the same row indicate significant difference ($p \leq 0.05$).

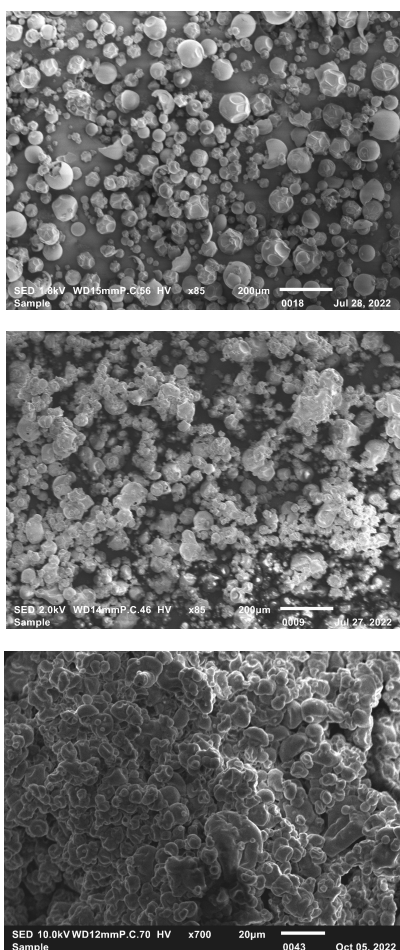


Figure 2. Particle microstructure of walnut flavor microcapsules for (a) M_{MG} ; (b) M_{WPC} and (c) M_{MG-WPC} .

(Beristain *et al.*, 2002), where mesquite gum was utilized as wall material. On the other hand, the microstructure of M_{WPC} exhibited a smooth and spherical surface particle attributed to inherent globular protein properties. These properties enable the formation of a robust layer that permits the encapsulation of walnut flavoring under spray drying conditions. This morphology has also been noted in microcapsules containing blackberry juice (Díaz *et al.*, 2015), vitamin D3 (Jafari *et al.*, 2019), and Persimmon pulp powders (Du *et al.*, 2014), where WPC was used as wall material. While M_{MG-WPC} microcapsules showed a composite microstructure by both spherical and agglomerated particles, they displayed a smooth surface with some dents. These features are representative of the microstructure resulting from the application of WPC and mesquite gum together as wall materials. Similar morphology has been documented in cocoa liquor microcapsules (Calva-Estrada *et al.*, 2019) and *Hybiscus sabdariffa* microcapsules (Ochoa-Velasco *et al.*, 2017) where combinations of WPC and mesquite gum were used as wall materials. Therefore, WPC and mesquite gum are excellent encapsulating biopolymers, serving as effective wall materials that protect walnut flavoring in a powdered form. Their ability to develop tunable microstructure by designing appropriate WPC-MG blends, plays a pivotal role in enhancing the flavor encapsulation under the spray drying conditions investigated in this study (Ordoñez-Eraso & Herrera, 2014; Rostamabadi *et al.*, 2022).

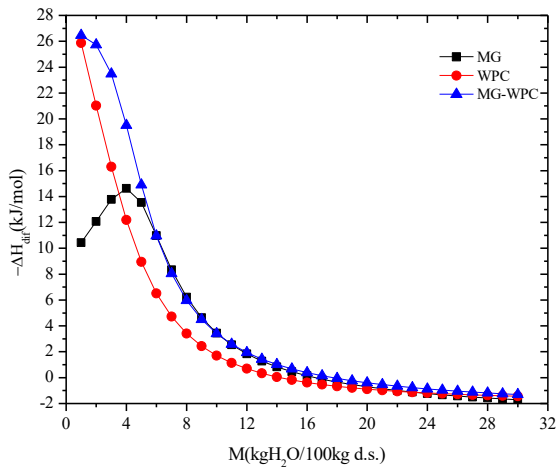


Figure 3. Differential enthalpy as a function of moisture content of walnut flavor microcapsules for (a) M_{MG} ; (b) M_{WPC} and (c) M_{MG-WPC} .

3.3 Differential thermodynamic properties of the microcapsules

Fig. 3 shows the differential enthalpy curves for the three microcapsules systems, revealing a significant difference between M_{MG} microcapsules and the other systems. In M_{WPC} and M_{MG-WPC} at low moisture contents, more negative enthalpy values were observed, this behavior can be attributed to hydrophobic groups in protein because water molecules require more energy to bind these solids. Then, when moisture content increased, differential enthalpy decreased due to less presence of active sites available and less energy of water molecules required to be adsorbed in multilayer formation. (Collazos-Escobar *et al.*, 2022; De Araújo & Da Silva-Pena, 2022). On the other hand, for M_{MG} microcapsules, the differential enthalpy curve exhibited distinct pattern at the beginning as moisture content increased, enthalpy values increased; an endothermic causes this process due to microcapsule's swelling that exposed new sites favoring adsorption of water molecules into monolayer until the reaching of a maximum differential enthalpy (14.64 kJ/mol) which is significantly minor than maximum enthalpy values of the other systems (25.86 and 26.47 kJ/mol for M_{WPC} and M_{MG-WPC} , respectively). Subsequently, with moisture content increasing, differential enthalpy values gradually decreased; this is attributed to multilayer formation and less availability of adsorption active sites (Velázquez-Gutiérrez *et al.*, 2015). Differences between enthalpy values of M_{WPC} and M_{MG-WPC} compared to enthalpy values of M_{MG} suggest that this last system leads to an encapsulation process relatively easy, which has implications for the design and operation of the drying equipment (De Araújo & Da Silva-Pena, 2022). Similar results have been reported by Bonilla *et al.* (2010) in canola oil

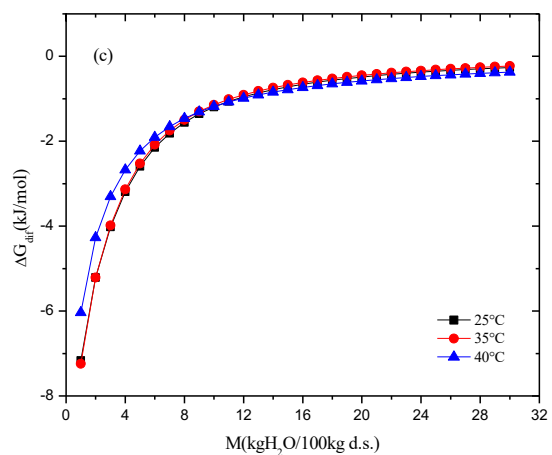
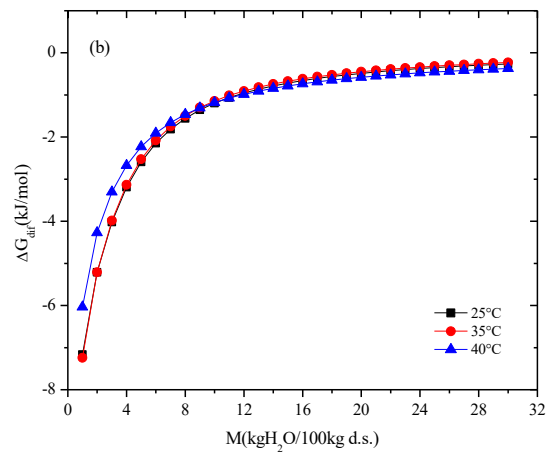
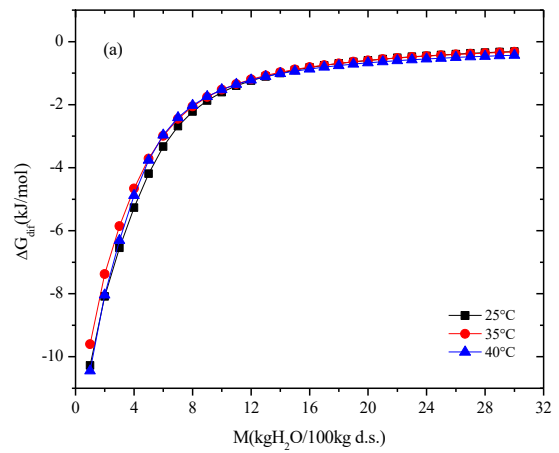


Figure 4. Differential free Gibbs energy as a function of moisture content of walnut flavor microcapsules for (a) M_{MG} ; (b) M_{WPC} and (c) M_{MG-WPC} .

microcapsules formed with soy protein isolate, MG and WPC, highlighting higher enthalpies in WPC-based systems compared to those formed with MG.

Fig. 4 shows the differential Gibbs free energy for the three types of microcapsules, this is a parameter related to the spontaneity of water sorption

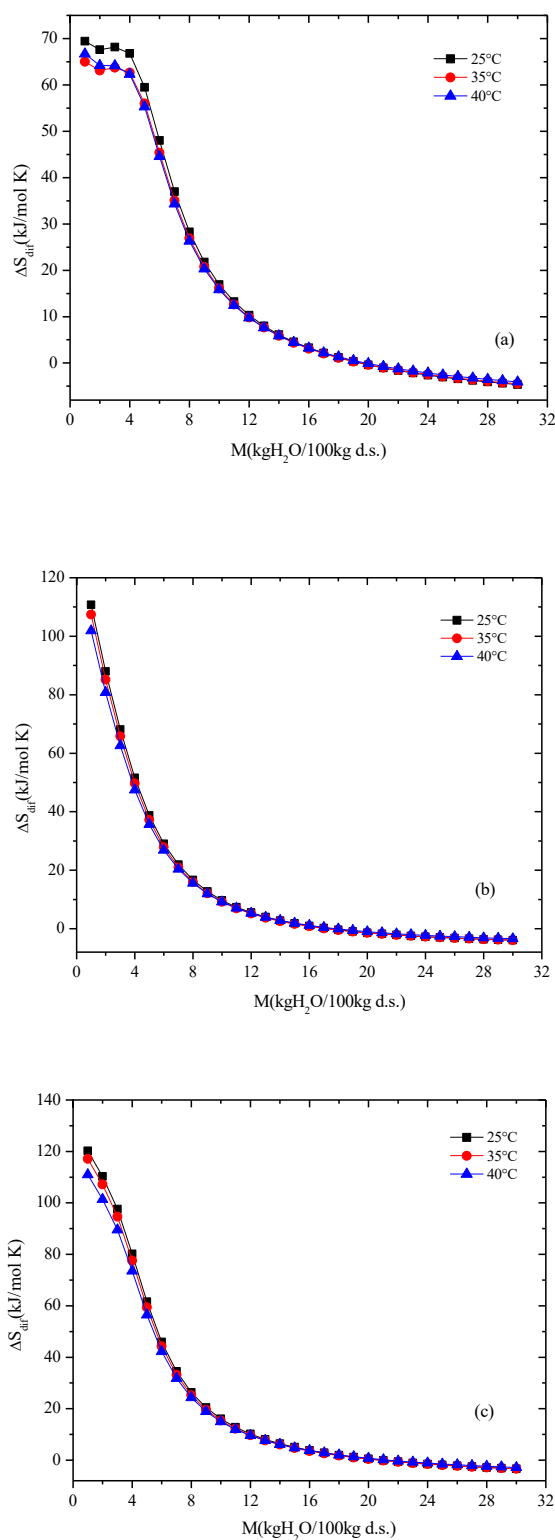


Figure 5. Differential entropy as a function of moisture content of walnut flavor microcapsules for (a) M_{MG} ; (b) M_{WPC} and (c) M_{MG-WPC} .

and the affinity between water and microcapsules. For the microcapsules evaluated in this work, all ΔG values were negative and very close to each other in the temperature range studied, indicating a spontaneous sorption process (De Araújo & Da Silva-

Pena, 2022). Rizvi (1995) explained that when the sorption process is spontaneous, strong intermolecular bonds (interactions) related to the enthalpy occur, which led to greater reduction in the configurational freedom of water molecules and therefore to greater order of the adsorbent-adsorbate system.

In the region where the moisture content of the monolayer is located (~ 4 - 5 kg $H_2O/100$ kg d.s.), the M_{MG} microcapsules showed the most negative values of ΔG , suggesting that the structure of the adsorbent that is form favored the spontaneity of the process, compared to the other two microencapsulated systems. Another factor that is possibly favoring the spontaneity of the process in this system is that the mesquite gum has a higher degree of hygroscopicity compared to the protein, making it easier for water molecules to adsorb on the surface of the solids (Collazos-Escobar *et al.*, 2022). As depicted in Figure 4, as the equilibrium moisture content increased, ΔG curves tended to zero. This behavior can be explained by the diminishing availability of available sorption sites at higher moisture contents (Collazos-Escobar *et al.*, 2022).

Fig. 5 displays the differential sorption entropy (ΔS_{dif}) behavior as a function of equilibrium moisture content for the three types of microcapsules. This figure shows that the values of ΔS_{dif} do not depend on temperature. The above can be explained in terms of the fact that the temperature range used did not favor the water molecules to have a high kinetic energy, which favored greater structural stability at the water-food matrix interface.

On the other hand, in the case of the three microencapsulated systems, ΔS_{dif} showed a strong dependence on the moisture content below 18 kg $H_2O/100$ kg d.s. presenting an exponential trend similar to that exhibited by differential enthalpy. The observed increase in ΔS_{dif} is attributed to the increase in the intensity of moisture sorption as the moisture content is lower. Since differential entropy describes the degree of disorder and randomness of the movement of water molecules, this thermodynamic parameter indicates the degree of irregularity in the adsorption process, so it can be said that as the moisture content in the microcapsules is lower, there will be greater irregularity in the adsorption process because new water molecules will be adsorbed by the solid at the same hydration level (Pérez-Alonso *et al.*, 2006).

3.4 Compensation theory

Fig. 6 presents the profiles for differential entropy *versus* differential enthalpy for the microcapsule systems. A linear correlation between both variables was observed for (a) M_{MG} , (b) M_{WPC} , and (c) M_{MG-WPC} microcapsules at temperatures of 25, 35, and 40 °C when the moisture content varied between

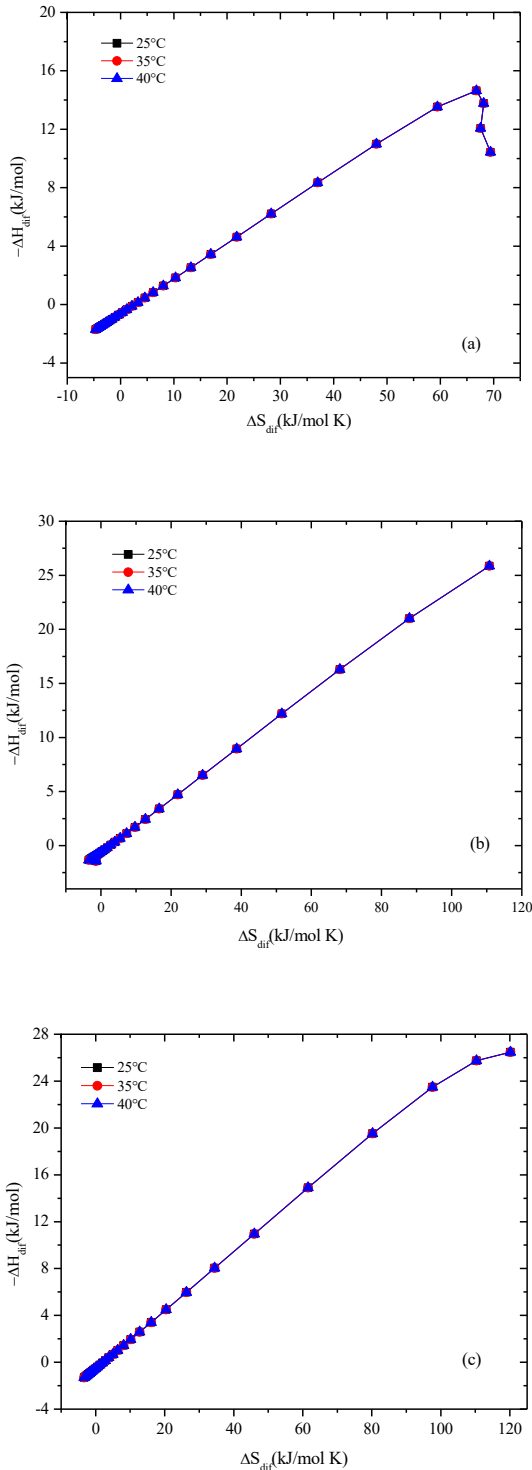


Figure 6. Differential enthalpy–integral entropy compensation for water sorption of walnut flavor microcapsules for (a) M_{MG} ; (b) M_{WPC} and (c) M_{MG-WPC} .

1 to 30 kg $H_2O/100$ kg d.s. This trend is identified as the compensation theory in thermodynamic terms, proving to be a more suitable approach to analyze the moisture adsorption process in the transition state (Cheng *et al.*, 2023). This study reveals a thermodynamic compensation phenomenon in walnut flavor microcapsules that takes place when changes

in the entropy and enthalpy values get an equilibrium state, exhibiting a linear relationship, which is related to the formation of new chemical bonds that produce more stable (less energetic) and more ordered microcapsules (less entropic). These results are also related to isokinetic temperature, moisture content and water activity values during the sorption process of microcapsules (Garvín *et al.*, 2017; Iglesias *et al.*, 2022). In this study, the sorption process of water molecules demonstrates an entropy-driven nature within the moisture content range from 1 to 30 kg $H_2O/100$ kg d.s., approximately.

The micropores of walnut flavor microcapsules contribute to enhancing the sorption process of water molecules driven by entropy. The free energy change obtained under these study conditions indicates the affinity of water-adsorbent in microcapsules as a criterion of entropy spontaneous process ($-\Delta G$), while enthalpic process ($+\Delta G$) is a non spontaneous process under a thermodynamic point of view (Azura & Beristain, 2006; Cheng *et al.*, 2023). This thermodynamic behavior related to compensation theory, has also been identified in Allspice essential oil (Sánchez-Sáenz *et al.*, 2011), borjón fruit (Rodríguez-Bernal *et al.*, 2015), in taro starch (Hoyos-Leyva *et al.*, 2018), in sesame oil hydrogel (Velázquez-Gutiérrez *et al.*, 2021), and in microalgae powders (Cheng *et al.*, 2023).

3.5 Sorption properties of microcapsules

The surface area of sorption and pore radius are some of the sorption properties relevant to food stability, as they directly impact the number of water molecules interacting with the active sites within the food matrix.

Table 2 shows the values for sorption surface area (S_0) of all microcapsules at the three different temperatures. In general, this parameter tends to decrease when temperature arises; this is attributed to the physical and chemical changes induced by temperature that reduce the available active sites for hydrophilic binding (Arslan-Tontul, 2021; Rosa *et al.*, 2021; Alpizar-Reyes *et al.*, 2017; Velázquez-Gutiérrez *et al.*, 2015). Notably, higher S_0 values were obtained for M_{MG} compared to the other two microencapsulated systems. The above indicates a more significant microporous structure where the surface interaction, hydrophilicity, structure and chemical composition of M_{MG} affect the water sorption capacity and lead to increase adsorption surface, which is usual in food matrices with a high carbohydrate content (Arslan-Tontul, 2021; Velázquez-Gutiérrez *et al.*, 2015).

Pore radius values for all walnut flavor microcapsules ranged from 0.63 to 12.65 nm (Figure 7), corresponding to both micropores (< 2 nm) and mesopores (2-50 nm) in agreement with the

Table 2. Surface area of sorption (m^2/g) for walnut flavor microcapsules.

| | 25 °C | 35 °C | 40 °C |
|---------------------|-----------------------------|------------------------------|-----------------------------|
| M_{MG} | $193.21 \pm 7.2^{\text{a}}$ | $184.16 \pm 6.9^{\text{ab}}$ | $164.05 \pm 6.5^{\text{b}}$ |
| M_{WPC} | $172.31 \pm 5.3^{\text{a}}$ | $163.63 \pm 5.1^{\text{ab}}$ | $167.72 \pm 5.6^{\text{b}}$ |
| $M_{\text{MG-WPC}}$ | $172.12 \pm 5.5^{\text{b}}$ | $164.93 \pm 4.8^{\text{b}}$ | $145.18 \pm 4.2^{\text{b}}$ |

*MG: Mesquite gum; WPC: Whey protein concentrate.

**Results are presented as means \pm SD ($n=3$).

***Values with different letters in the same row indicate significant difference ($p \leq 0.05$).

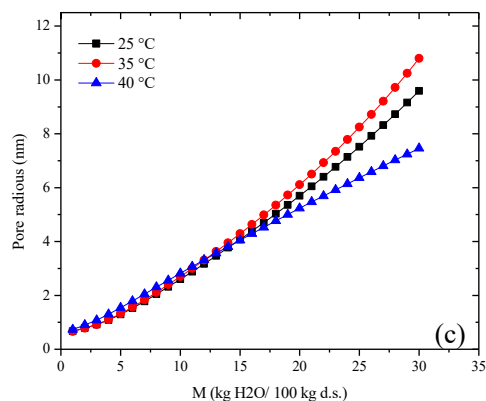
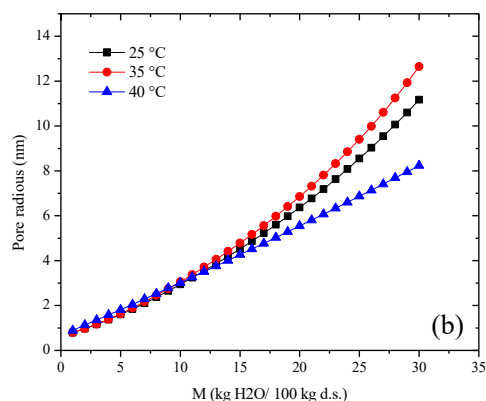
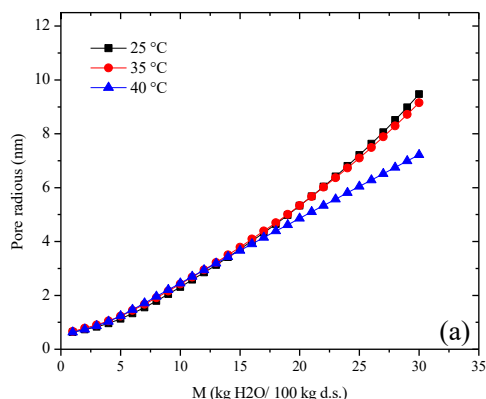


Figure 7. Pore radius as a function of moisture content of walnut flavor microcapsules for (a) M_{MG} ; (b) M_{WPC} and (c) $M_{\text{MG-WPC}}$.

International Union of Pure and Applied Chemistry (IUPAC) (Alpizar-Reyes *et al.*, 2017; Velázquez-Gutiérrez *et al.*, 2015). The moisture content in the monolayer region (4-5 kg $\text{H}_2\text{O}/100$ kg d.s.) is where the strongest interactions between the adsorbent and the adsorbate occur. As can be seen in Figure 7, it corresponds to the microporous zone of the microcapsules. As the moisture content increases, the interactions begin to decrease due to the formation of multilayers, which occurs in the mesoporous zone and the condensation regions (Monte *et al.*, 2018).

Table 3 displays the Dubinin-Radushkevich model for walnut flavor microcapsules; this model helps to characterize the micropore region. It was observed that the moisture content corresponding to the micropore volume (M_{0D}) decreased as temperature increased, the values were in the range of 1.376 to 3.967 kg $\text{H}_2\text{O} / 100$ kg d.s., which indicates that the formation of the monolayer occurs after all micropores are filled. As temperature increases, M_{0D} decreases, probably due to an increase in kinetic energy of water molecules with temperature or the contraction of the biopolymeric matrix of the microcapsules. On the other hand, the different porous structures of the three types of microcapsules have presented diffusion mechanisms. An entropy-driven sorption process occurred when, in the microporous region (<2 nm), there were interactions between the diffusing molecule and the pore walls; while in the mesoporous region, an enthalpy-driven process occurred where surface forces and capillary forces were important (Fletcher & Thomas, 2000; Azuara & Beristain, 2006).

Conclusion

In this research, walnut flavor microcapsules were evaluated using three different wall materials, mesquite gum (M_{MG}), whey protein (M_{WPC}) and their mixture ($M_{\text{MG-WPC}}$) 1:1 mass ratio, on their moisture sorption capacity and thermodynamic properties across temperatures of 25, 35 and 40°C. All three microcapsules' systems presented sigmoidal type II curves indicative of water adsorption occurring in both monolayer and multilayer mechanisms

Table 3. Estimated Parameters of Dubinin-Radushkevich model for walnut flavor microcapsules.

| System | Parameters | 25 °C | 35 °C | 40 °C |
|---------------------|-----------------|---------------------------|----------------------------|---------------------------|
| M _{MG} | M _{0D} | 3.967 ± 0.23 ^a | 3.613 ± 0.22 ^{ab} | 3.304 ± 0.21 ^b |
| | <i>b</i> | 0.719 ± 0.12 ^a | 0.754 ± 0.111 ^a | 0.820 ± 0.13 ^b |
| | R ² | 0.992 | 0.990 | 0.994 |
| M _{WPC} | M _{0D} | 2.164 ± 0.22 ^a | 1.937 ± 0.25 ^{ab} | 1.376 ± 0.23 ^b |
| | <i>b</i> | 0.938 ± 0.14 ^a | 0.996 ± 0.12 ^a | 1.198 ± 0.12 ^b |
| | R ² | 0.980 | 0.975 | 0.992 |
| M _{MG-WPC} | M _{0D} | 3.440 ± 0.26 ^a | 3.195 ± 0.22 ^{ab} | 2.328 ± 0.24 ^b |
| | <i>b</i> | 0.756 ± 0.13 ^a | 0.764 ± 0.12 ^a | 0.947 ± 0.14 ^b |
| | R ² | 0.996 | 0.984 | 0.997 |

*MG: Mesquite gum; WPC: Whey protein concentrate; M_{0D}: Moisture content corresponding to the micropore volume (kg water/100 kg d.s; *b*: D-R model constant; a_w: Water activity; R²: Coefficient of linear determination.

**Results are presented as means ± SD (n=3).

***Values with different letters in the same row indicate significant difference (p<0.05).

on their porous surfaces. However, M_{MG} had a greater moisture adsorption capacity, showcasing stronger adsorbent-adsorbate interactions due to its greater hygroscopicity. Additionally, M_{MG} did not exhibit agglomeration as occurred with M_{WPC} and M_{MG-WPC}. The M_{MG} also showed the lowest values of differential enthalpy and entropy, favoring the dehydration process and indicating a more ordered arrangement of water molecules, contributing to enhanced system stability. Likewise, the M_{MG} had the largest sorption surface area due to its microporous structure, facilitating and increased water sorption process and resulting in higher values of moisture content in the monolayer. All three microcapsules' systems displayed negative free energy, indicating a spontaneous moisture adsorption process. In general, the three microcapsules' systems can stabilize the walnut flavoring. However, the slight differences in their moisture sorption capacity and thermodynamic properties under specific moisture and temperature conditions suggest distinct stabilization mechanisms emphasizing the critical role of selecting a suitable wall material to ensure optimal protection for walnut flavoring throughout its shelf life.

Acknowledgements

The authors wish to acknowledge the financial support of this research to the Universidad Autónoma del Estado de México through grant 7043/2024 CIB.

Nomenclature

| | |
|----------------|--|
| a _w | Water activity |
| A _w | Area of a water molecule (1.06 × 10 ⁻¹⁹ m ²) |
| <i>b</i> | Constant related to the microporous structure of the adsorbent in Dubinin-Radushkevich model |
| C, K | GAB model coefficients |

| | |
|-----------------------|---|
| <i>E</i> | Minimum means absolute percentage error (%) |
| <i>M</i> | Equilibrium moisture content (kg water-100 kg ⁻¹ dry solid) |
| M _{Ei} | The predicted moisture content at observation <i>i</i> |
| M _i | The moisture content at observation <i>i</i> |
| M _{MG} , | Microcapsules code |
| M _{MG-WPC} , | |
| M _{WPC} | |
| M _{0D} | Amount of moisture adsorbed (kg water-100 kg ⁻¹ dry solid) corresponding to the micropore volume in Dubinin-Radushkevich model |
| M ₀ | Monolayer moisture content (kg water-100 kg ⁻¹ dry solid) |
| M _w | Molecular weight of water (18 kg·mol ⁻¹) |
| n _i | Total number of isotherms used |
| n _s | Number of observations |
| N ₀ | Avogadro number (6.0 × 10 ²³ molecules·mol ⁻¹) |
| q _{st} | Net isosteric heat of sorption (kJ·mol ⁻¹) |
| <i>R</i> | Universal gas constant (kJ·mol ⁻¹ K ⁻¹) |
| R _p | Pore radius (nm) |
| r _c | Critical radius (m) |
| S ₀ | Sorption surface area (m ² ·g ⁻¹) |
| <i>t</i> | Multilayer thickness (nm) |
| <i>T</i> | Temperature (K) |
| T _{hm} | Harmonic mean temperature (K) |
| T _β | Isokinetic temperature (K) |
| V _M | Molar volume of sorbate (m ³ ·mol ⁻¹) |
| | <i>Greek symbols</i> |
| ΔG _β | Free energy at T _β (kJ·mol ⁻¹) |
| ΔH _{dif} | Molar differential enthalpy (kJ·mol ⁻¹ K ⁻¹) |
| σ | Surface tension (N·m ⁻¹) |
| ΔS _{dif} | Molar differential entropy (kJ·mol ⁻¹ K ⁻¹) |

References

- Alpizar-Reyes, E., Carrillo-Navas, H., Romero-Romero, R., Varela-Guerrero, V., Alvarez-Ramírez, J., & Pérez-Alonso, C. (2017). Thermodynamic sorption properties and glass transition temperature of tamarind seed mucilage (*Tamarindus indica* L.). *Food and Bioprocess Processing*, 101, 166–176. <http://dx.doi.org/10.1016/j.fbp.2016.11.006>
- Arslan-Tontul, S. (2021). Moisture sorption isotherm and thermodynamic analysis of quinoa grains. *Heat and Mass Transfer*, 57, 543–550. <https://doi.org/10.1007/s00231-020-02978-8>
- Azuara, E., & Beristain, C. I., (2006). Enthalpic and entropic mechanisms related to water sorption of yogurt. *Drying Technology*, 24(11), 1501-1507. <https://doi.org/10.1080/07373930600961173>
- Beristain, C. I., Azuara, E., & Vernon-Carter, E. J. (2002). Effect of water activity on the stability to oxidation of spray-dried encapsulated orange peel oil using mesquite gum (*Prosopis juliflora*) as wall material. *Journal of Food Science*, 67, 206–211. <https://doi.org/10.1111/j.13652621.2002.tb11385.x>
- Bonilla, E., Azuara, E., Beristain, C. I., & Vernon-Carter, E. J. (2010). Predicting suitable storage conditions for spray-dried microcapsules formed with different biopolymer matrices. *Food Hydrocolloids*, 24(6-7), 633-640. <https://doi.org/10.1016/j.foodhyd.2010.02.010>
- Calva-Estrada, S. J., Lugo-Cervantes, E., & Jiménez-Fernández, M. (2019). Microencapsulation of cocoa liquor nanoemulsion with whey protein using spray drying to protection of volatile compounds and antioxidant capacity. *Journal of Microencapsulation*, 36(5), 447–458. <https://doi.org/10.1080/02652048.2019.1638463>
- Carneiro, H. C. F., Hoster, K., Reineccius, G., & Prata, A. S. (2022). Flavoring properties that affect the retention of volatile components during encapsulation process. *Food Chemistry X*, 13, 100230. <https://doi.org/10.1016/j.fochx.2022.100230>
- Cheng, X., Ling, P., Iqbal, M. S., Liu, F., Xu, J., & Wang, X. (2023). Water adsorption properties of microalgae powders: Thermodynamic analysis and structural characteristics. *Journal of Stored Products Research*, 101, 102093. <https://doi.org/10.1016/j.jspr.2023.102093>
- Chranioti, C., Nikoloudaki, A., & Tzia, C. (2015). Saffron and beetroot extracts encapsulated in maltodextrin, gum Arabic, modified starch and chitosan: Incorporation in a chewing gum system. *Carbohydrate Polymers*, 127, 252-263. <https://doi.org/10.1016/j.carbpol.2015.03.049>
- Collazos-Escobar, G. A., Gutiérrez-Guzmán, N., Váquiro-Herrera, H. A., Bon, J., & Garcia-Perez, J. V. (2022). Thermodynamic analysis and modeling of water vapor adsorption isotherms of roasted specialty coffee (*Coffea arabica* L. cv. Colombia). *LWT - Food Science and Technology*, 160, 113335. <https://doi.org/10.1016/j.lwt.2022.113335>
- Cortés-Camargo, S., Cruz-Olivares, J., Barragán-Huerta, B. E., Dublán-García, O., Román-Guerrero, A., & Pérez-Alonso, C. (2017). Microencapsulation by spray drying of lemon essential oil: Evaluation of mixtures of mesquite gum–nopal mucilage as new wall materials. *Journal of Microencapsulation*, 34(4), 395–407. <https://doi.org/10.1080/02652048.2017.1338772>
- De Araújo, A. L., & Da Silva-Pena, R. (2022). Moisture desorption behavior and thermodynamic properties of pulp and seed of jambolan (*Syzygium cumini*). *Heliyon*, 8(5), 09443. <https://doi.org/10.1016/j.heliyon.2022.e09443>
- Díaz, D. I., Beristain, C. I., Azuara, E., Luna, G., & Jiménez, M. (2015). Effect of wall material on the antioxidant activity and physicochemical properties *Ofrubus fruticosus* juice microcapsules. *Journal of Microencapsulation*, 32(3), 247–254. <https://doi.org/10.3109/02652048.2015.1010458>
- Drusch, S., & Berg, S. (2008). Extractable oil in microcapsules prepared by spray-drying: Localisation, determination and impact on oxidative stability. *Food Chemistry*, 109(1), 17-24. <https://doi.org/10.1016/j.foodchem.2007.12.016>
- Du, J., Ge, Z.-Z., Xu, Z., Zou, B., Zhang, Y., & Li, C.-M. (2014). Comparison of the efficiency of five different drying carriers on the spray drying of persimmon pulp powders. *Drying Technology*, 32(10), 1157–1166. <https://doi.org/10.1080/07373937.2014.886259>

- Espinosa-Andrews, H., Morales-Hernández, N., García-Márquez, E., & Rodríguez-Rodríguez, R. (2022). Development of fish oil microcapsules by spray drying using mesquite gum and chitosan as wall materials: Physicochemical properties, microstructure, and lipid hydroperoxide concentration. *International Journal of Polymeric Materials and Polymeric Biomaterials*, 72(8), 646–655. <https://doi.org/10.1080/00914037.2022.2042289>
- Feng, T., Wang, H., Wang, K., Liu, Y., Rong, Z., Ye, R., Zhuang, H., Xu, Z., & Sun, M. (2018). Preparation and structural characterization of different amylose–flavor molecular inclusion complexes. *Starch-Stärke*, 70(1–2). <https://doi.org/10.1002/star.201700101>
- Fletcher, A. J., & Thomas, K.M. (2000). Compensation effect for the kinetics of adsorption/desorption of gases/vapors on microporous carbon materials. *Langmuir*, 16, 6253–6266. <https://doi.org/10.1021/la9916528>
- Fuciños, C., Míguez, M., Fuciños, P., Pastrana, L. M., Rúa, M. L., & Vicente, A. A. (2017). Creating functional nanostructures: Encapsulation of caffeine into α -lactalbumin nanotubes. *Innovative Food Science & Emerging Technologies*, 40, 10–17. <https://doi.org/10.1016/j.ifset.2016.07.030>
- Gallegos-Marin, I., Méndez-Lagunas, L. L., Rodríguez-Ramírez, J., & Martínez-Sánchez, C. E. (2016). Structural properties changes during osmotic drying of plantain (*Musa paradisiaca* AAB) and its role on mass transfer. *Revista Mexicana de Ingeniería Química*, 15(2), 441–456.
- Garvín, A., Ibarz, R., & Ibarz, A. (2017). Kinetic and thermodynamic compensation. A current and practical review for Foods. *Food Research International*, 96, 132–153. <https://doi.org/10.1016/j.foodres.2017.03.004>
- Hernández-Carrillo, J. G., Mújica-Paz, H., Welti-Chanes, J., Spatafora-Salazar, A. S., & Valdez-Fragoso, A. (2019). Sorption behavior of citric pectin films with glycerol and olive oil. *Revista Mexicana de Ingeniería Química*, 18(2), 487–500. <https://doi.org/10.24275/uam/izt/dcbi/revmexingquim/2019v18n2/Hernandez>
- Hoyos-Leyva, J. D., Bello-Pérez, L. A., Agama-Acevedo, E., & Alvarez-Ramirez, J. (2018). Thermodynamic analysis for assessing the physical stability of core materials microencapsulated in taro starch spherical aggregates. *Carbohydrate Polymers*, 197, 431–441. <https://doi.org/10.1016/j.carbpol.2018.06.012>
- Iglesias, H. A., Baeza, R., & Chirife, J. (2022). A survey of temperature effects on GAB monolayer in foods and minimum integral entropies of sorption: A review. *Food and Bioprocess Technology*, 15(4), 717–733. <https://doi.org/10.1007/s11947-021-02740-w>
- Jafari, S. M., Masoudi, S., & Bahrami, A. (2019). A Taguchi approach production of spray-dried whey powder enriched with nanoencapsulated vitamin D3. *Drying Technology*, 37(16), 2059–2071. <https://doi.org/10.1080/07373937.2018.1552598>
- Kim, E. H. J., Paredes, D., Motoi, L., Eckert, M., Wadamori, Y., Tartaglia, J., Green, C., Hedderley, D. I., & Morgenstern, M. P. (2019). Dynamic flavor perception of encapsulated flavors in a soft chewable matrix. *Food Research International*, 123, 241–250. <https://doi.org/10.1016/j.foodres.2019.04.038>
- Krug, R. R., Hunter, W. G., & Grieger, R. A. (1976a). Enthalpy–entropy compensation 1. Some fundamental statistical problems associated with the Van't Hoff and Arrhenius data. *Journal of Physical Chemistry*, 80, 2335–2341. <https://doi.org/10.1021/j100562a006>
- Krug, R.R., Hunter, W.G., & Grieger, R.A., (1976b). Enthalpy–entropy compensation 2. Separation of the chemical from the statistical effect. *Journal of Physical Chemistry*, 80, 2342–2351. <https://doi.org/10.1021/j100562a007>
- Monte, M.L., Moreno, M.L., Senna, J., Arrieche, L.S., & Pinto, L.A.A. (2018). Moisture sorption isotherms of chitosan-glycerol films: Thermodynamic properties and microstructure. *Food Bioscience*, 22, 170–177. <https://doi.org/10.1016/j.fbio.2018.02.004>
- Ocieczek, A., Mesinger, D., & Toczek, H. (2022). Hygroscopic properties of three cassava (*Manihot esculenta* Crantz) starch products: application of BET and GAB models. *Foods*, 11(13), 1966. <https://doi.org/10.3390/foods11131966>
- Ochoa-Velasco, C. E., Salazar-González, C., Cid-Ortega, S., & Guerrero-Beltrán, J. A. (2017). Antioxidant characteristics of extracts of *Hibiscus sabdariffa* calyces encapsulated with

- mesquite gum. *Journal of Food Science and Technology*, 54(7), 1747–1756. <https://doi.org/10.1007/s13197-017-2564-1>
- Ordoñez-Eraso M. & Herrera A. (2014). Use of Starches and Milk Proteins in Microencapsulation, *International Journal of Vegetable Science*, 20(4), 289-304. <https://doi.org/10.1080/19315260.2013.803181>
- Osorio-Tellez, A., Pedroza-Islas, R., & Pérez-Alonso, C. (2021). Prediction of storage stability parameters of spray dried powders of maltodextrins and corn syrups with different levels of hydrolysis (conversion). *Revista Mexicana de Ingeniería Química*, 20(2), 679-696. <https://doi.org/10.24275/rmiq/Alim2136>
- Pascual-Pineda, L. A., Alamilla-Beltrán, L., Gutiérrez-López, G. F., Azuara, E., & Flores-Andrade, E. (2017). Prediction of storage conditions of dehydrated foods from a water vapor adsorption isotherm. *Revista Mexicana de Ingeniería Química*, 16(1), 207-220. <https://doi.org/10.24275/rmiq/Alim817>
- Pérez-Alonso, C., Beristain, C. I., Lobato-Calleros, C., Rodríguez-Huezo, M. E., & Vernon-Carter, E. J. (2006). Thermodynamic analysis of the sorption isotherms of pure and blended carbohydrate polymers. *Journal of Food Engineering*, 77, 753-760. <https://doi.org/10.1016/j.jfoodeng.2005.08.002>
- Premjit, Y., Pandhi, S., Kumar, A., Rai, D. C., Duary, R. K., & Mahato, D. K. (2022). Current trends in flavor encapsulation: A comprehensive review of emerging encapsulation techniques, flavour release, and mathematical modelling. *Food Research International*, 151, 110879. <https://doi.org/10.1016/j.foodres.2021.110879>
- Quirijns, E. J., Van Boxtel, A. J., Van Loon, W. K., & Van Straten, G. (2005). Sorption isotherms, GAB parameters and isosteric heat of sorption. *Journal of the Science of Food and Agriculture*, 85(11), 1805-1814. <https://doi.org/10.1002/jsfa.2140>
- Rizvi, S.S.H. (1986). Engineering Properties of Foods. In M.A. Rao & S.S.H. Rizvi (Eds), *Thermodynamic Properties of Foods in Dehydration* (pp. 133-214). New York: Marcel Dekker Inc.
- Rizvi, S.S.H. (1995). Engineering Properties of Foods. In M.A. Rao & S.S.H. Rizvi (Eds), *Thermodynamic Properties of Foods in Dehydration* (pp. 223-309). New York: Academic Press.
- Rodríguez-Bernal, J. M., Flores-Andrade, E., Lizarazo-Morales, C., Bonilla, E., Pascual-Pineda, L. A., Gutiérrez-López, G., & Quintanilla-Carvajal, M. X. (2015). Moisture adsorption isotherms of the Borojó Fruit (borojoa patinoi. Cuatrecasas) and gum arabic powders. *Food and Bioproducts Processing*, 94, 187–198. <https://doi.org/10.1016/j.fbp.2015.03.004>
- Rosa, D. P., Evangelista, R. R., Machado, A. L. B., Sanches, M. A. R., & Telis-Romero, J. (2021). Water sorption properties of papaya seeds (*Carica papaya* L.) formosa variety: An assessment under storage and drying conditions. *LWT - Food Science and Technology*, 138, 110458. <https://doi.org/10.1016/j.lwt.2020.110458>
- Rostamabadi, M. M., Falsafi, S. R., Nishinari, K., & Rostamabadi, H. (2022). Seed gum-based delivery systems and their application in encapsulation of bioactive molecules. *Critical Reviews in Food Science and Nutrition*, 63(29),9937-9960. <https://doi.org/10.1080/10408398.2022.2076065>
- Saffarionpour, S. (2019). Nanoencapsulation of hydrophobic food flavor ingredients and their cyclodextrin inclusion complexes. *Food and Bioprocess Technology*, 12(7), 1157–1173. <https://doi.org/10.1007/s11947-019-02285-z>
- Saifullah, M., Shishir, M. R. I., Ferdowsi, R., Tanver Rahman, M. R., & Van Vuong, Q. (2019). Micro and nano encapsulation, retention and controlled release of flavor and aroma compounds: A critical review. *Trends in Food Science & Technology*, 86, 230–251. <https://doi.org/10.1016/j.tifs.2019.02.030>
- Saini, A., Panwar, D., Panesar, P. S., & Bera, M. B. (2020). Encapsulation of functional ingredients in lipidic nanocarriers and antimicrobial applications: A review. *Environmental Chemistry Letters*, 19, 1107–1134. <https://doi.org/10.1007/s10311-020-01109-3>
- Samakradhamrongthai, R. S., Angeli, P. T., Kopermsub, P., & Utama-Ang, N. (2019). Optimization of gelatin and gum arabic capsule infused with pandan flavor for multi-core flavor powder encapsulation. *Carbohydrate Polymers*, 226, 115262. <https://doi.org/10.1016/j.carbpol.2019.115262>

- Sánchez-Sáenz, E. O., Pérez-Alonso, C., Cruz-Olivares, J., Román-Guerrero, A., Báez-González, J. G., & Rodríguez-Huezo, M. E. (2011). Establishing the most suitable storage conditions for microencapsulated allspice essential oil entrapped in blended biopolymers matrices. *Drying Technology*, 29(8), 863–872. <https://doi.org/10.1080/07373937.2010.545495>
- Shanker, N., Kumar, M. M., Juvvi, P., & Debnath, S. (2019). Moisture sorption characteristics of ready-to-eat snack food enriched with purslane leaves. *Journal of Food Science and Technology-Mysore*, 56(4), 1918–1926. <https://doi.org/10.1007/s13197-019-03657-1>
- Silva, K. S., Polachini, T. C., Luna-Flores, M., Luna-Solano, G., Resende, O., & Telis-Romero, J. (2021). Sorption isotherms and thermodynamic properties of wheat malt under storage conditions. *Journal of Food Process Engineering*, 44(9), 13784. <https://doi.org/10.1111/jfpe.13784>
- Singh, R. R. B., Rao, K. H., Anjaneyulu, A. S. R., & Patil, G. R. (2001). Moisture sorption properties of smoked chicken sausages from spent hen meat. *Food Research International*, 34 (2–3), 143–148. [https://doi.org/10.1016/S0963-9969\(00\)00145-9](https://doi.org/10.1016/S0963-9969(00)00145-9)
- Soleimanifard, S., & Hamdami, N. (2018). Modelling of the sorption isotherms and determination of the isosteric heat of split pistachios, pistachio kernels and shells. *Czech Journal of Food Sciences*, 36(3), 268–275. <https://doi.org/10.17221/460/2016-cjfs>
- Sonwane, C. G., & Bhatia, K. (2000). Characterization of pore size distributions of mesoporous materials from adsorption isotherms. *Journal of Physical Chemistry B*, 104, 9099–9110. <https://doi.org/10.1021/jp000907j>
- Stępień, A., Witczak, M., & Witczak, T. (2020). Moisture sorption characteristics of food powders containing freeze dried avocado, maltodextrin and inulin. *International Journal of Biological Macromolecules*, 149, 256–261. <https://doi.org/10.1016/j.ijbiomac.2020.01.154>
- Sultana, A., Tanaka, Y., Fushimi, Y., & Yoshii, H. (2018). Stability and release behavior of encapsulated flavor from spray-dried *Saccharomyces cerevisiae* and maltodextrin powder. *Food Research International*, 106, 809–816. <https://doi.org/10.1016/j.foodres.2018.01.059>
- Timmermann, E.O., Chirife, J., & Iglesias, H.A. (2001). Water sorption isotherms of foods and foodstuffs: BET or GAB parameters? *Journal of Food Engineering*, 48, 19–31. [https://doi.org/10.1016/S0260-8774\(00\)00139-4](https://doi.org/10.1016/S0260-8774(00)00139-4)
- Timmermann, E.O. (1989). A BET-like three sorption stage isotherms. *Journal of Chemical Society Faraday Transactions I*, 85, 1631–1645. <https://doi.org/10.1039/F19898501631>
- Velázquez-Gutiérrez, S. K., Alpizar-Reyes, E., Guadarrama-Lezama, A. Y., Báez-González, J. G., Alvarez-Ramírez, J., & Pérez-Alonso, C. (2021). Influence of the wall material on the moisture sorption properties and conditions of stability of sesame oil hydrogel beads by ionic gelation. *LWT - Food Science and Technology*, 140, 110695. <https://doi.org/10.1016/j.lwt.2020.110695>
- Velázquez-Gutiérrez, S. K., Figueira, A. C., Rodríguez-Huezo, M. E., Román-Guerrero, A., Carrillo-Navas, H., & Pérez-Alonso, C. (2015). Sorption isotherms, thermodynamic properties and glass transition temperature of mucilage extracted from chia seeds (*Salvia hispanica* L.). *Carbohydrate Polymers*, 121, 411–419. <https://doi.org/10.1016/j.carbpol.2014.11.068>
- Włodarczyk-Stasiak, M., & Jamroz, J. (2008). Analysis of sorption properties of starch-protein extrudates with the use of water vapour. *Journal of Food Engineering*, 85(4), 580–589. <https://doi.org/10.1016/j.jfoodeng.2007.08.019>